

A Simulation-Based Testing to Evaluate and Improve a Radar Sensor Performance in a Use Case of Highly Automated Driving Systems

Marzana Khatun¹ ^a, Mark Liske¹, Rolf Jung¹ and Michael Glaß² ^b

¹Institute for Advanced Driver Assistance Systems and Connected Mobility, Kempten University of Applied Sciences, BahnhofstraSe 61, Kempten (Allgäu), Germany

²Institute of Embedded Systems/Real-Time Systems, University of Ulm, Albert-Einstein-Allee 11, Ulm, Germany

Keywords: HAD, SOTIF, FuSa, MATLAB, Radar Sensor.

Abstract: The development of Highly Automated Driving (HAD) systems is necessary for automated vehicles in terms of various complex functionalities. HAD systems consist of complex structures containing different types of sensors. The functionality of HAD systems needs to be tested to ensure the overall safety of automated vehicles. Methods such as real-world testing require a large number of driving miles and are enormously expensive and time-consuming. Therefore, simulation-based testing is widely accepted and applicable in the development of HAD systems, including sensor performance improvement. In order to identify the functional insufficiency of such sensors that affect the safety of HAD systems, it is critical to test these sensors extensively under a variety of conditions such as, road types, environment and traffic situations. Based on this motivation, the main contributions of this paper are as follows: First, a simulation-based test concept of radar sensors with methods for the Safety Of the Intended Functionality (SOTIF) use case is presented. Second, a specific radar effect is evaluated through simulation-based testing of two different radar models to support and realize the sensor's functional insufficiency. Finally, the development of a filter is proposed to improve the sensor performance considering the radar specific multipath propagation effects.

1 INTRODUCTION

The development of Highly Automated Driving (HAD) systems depends not only on the vehicle's operational functions, but also on the perception of situations obtained by the support of sensors used in automated vehicles. The reliability of the HAD systems functionality depends on the perception of environment and driving situations (Berk et al., 2020). According to Society of Automotive Engineers (SAE), automation levels are divided into six levels from level 0 (*no driving automation*) to level 5 (*full driving automation*) (SAEJ3016, 2021). In this paper, HAD systems indicate the systems that are applicable to automation level 3 (*conditional driving automation*) to level 5 vehicles.

A concern has been raised in HAD systems development about incorrect situational awareness in terms of sensor's and algorithm's functional insufficiency (ISO21448, 2022; Becker et al., 2020). On the one hand, Functional Safety (FuSa) has targeted the op-

erational functions of HAD systems such as lateral and longitudinal vehicle control (ISO26262, 2018). On the other hand, Safety Of The Intended Functionality (SOTIF) has focused on the functional insufficiency that can lead to a hazardous situation or harm (ISO21448, 2022).

HAD systems consist of complex architectural structure considering the hardware, software, algorithms, interaction with human. The potential hazardous situations caused by the performance insufficiency of sensors are addressed in SOTIF, focusing on the triggering events that cause hazardous behaviors for specific use cases. HAD systems rely on sensor technology to predict the environment and situations. Based on this prediction, the systems make driving decisions (Khatun et al., 2020; Mazzega, 2019; Leither et al., 2020). Thus, the sensor model has a significant role in automated driving development, and further research and simulation-based testing are in demand (Khatun et al., 2021b; Khatun et al., 2021a). In this paper, simulation-based process is described for a radar sensor including the investigation of the performance and possible improvement is proposed by

^a  <https://orcid.org/0000-0002-3839-1575>

^b  <https://orcid.org/0000-0002-8006-8843>

developing a filter for a specific SOTIF related use case.

The structure of this paper is as follows: a brief description of HAD systems and sensor's functional insufficiency considering the available standards and techniques are stated in section 2. The sensor related activities and a specific use case are outlined in section 3 together with the sensor model architectures. Section 4 contains a description of the simulation-based testing approach and the test methods with the results. Finally, section 5 concluded the outcomes of this study and provides an outlook on further research aspects.

2 STATE-OF-THE-ART

Advanced driver assistance systems provide support to reduce the number of road accidents and increase human comfort. The automotive technologies are rapidly evolving in each stages of road vehicle safety. Now-a-days, new or adjusted methods and technologies have been applied in concept phase, development, production, operational, deployment of HAD systems (UL4600, 2022; IEC/TR63069, 2019; Valdez Banda and Goerlandt, 2018). HAD systems include several advanced driver assistance functions, such as automated driving from point A to point B without human intervention. In this work, for simplicity and easier expression, the term HAD systems has been used to define the vehicle systems used for the entire dynamic driving task in automation level 3 to level 5 (SAEJ3016, 2021).

Hazards caused by the malfunction behaviors of automotive Electrical and Electronic (E/E) elements are the prime focused of FuSa (ISO26262, 2018). Hazards originated from incorrect situational awareness and insufficient specification or performance insufficiency are covered by SOTIF (ISO21448, 2022). According to ISO 21448, SOTIF is defined as, *absence of unreasonable risk due to hazards resulting from functional insufficiencies of the intended functionality or its implementation*. Functional insufficiency reflects the limitation in technical capability of an E/E element or subsystems. The functional insufficiency can be known or unknown for a E/E elements (ISO21448, 2022). SOTIF focuses on the system behavior, the interaction with the driver as well as address foreseeable misuse by the driver or other people including risk mitigation approaches (Yu et al., 2022; Becker et al., 2020). Camera and LIDAR distortion phenomena as sensor imperfection that can cause malfunction behavior of HAD systems have been mentioned in (Martin et al., 2019). Further-

more, the highway chauffeur system is considered by NHTSA to analysis the SOTIF of lane centering and lane changing maneuvers of a generic Level 3 (Becker et al., 2020). These has been considered as a knowledge for radar sensor performance investigation and its improvement.

In HAD system radar has become one of the major sensors that has been applied in advanced functions such as collision avoidance, object detection of road and support in decision-making algorithms. Radar sensor has been used as a primary sensor in safety critical systems (Parker, 2017). The Radar (Radio Detection and Ranging) technology in HAD system is applied to detect and locate objects of interest. The objects of interest in automotive applications are road users such as ego-vehicle and/or other road users (pedestrian, leading/lagging vehicles motorcycles, trucks) including obstacles on the road for example guard rails. One other essential function of the radar is to determine the velocity of those objects relative to the radar sensor (Winner et al., 2015).

Besides the determination of the distance and velocity, the radar also can measure the angular position of the target relative to the position, where the radar sensor is located. The angular position can be determined due to the directive characteristics of the radar antenna (Schlager et al., 2020). By mixing the two received signals, the angular position can be determined due to the phase shift. A list of radar effects is as follows (Zhou et al., 2022; Schlager et al., 2020; Herz et al., 2019):

- Multipath propagation
- Weather and atmospheric attenuation
- Secondary surface effects of the radar signal.
- Inter-sensor-interference

The radar effects are classified into four areas of the resulting detection as, (i) False Negative, (ii) True Positive, (iii) False Positive, and (iv) True Negative. The area true positive has referred as the correct prediction of targets when its present. False positive has detected the prediction which are not real. Thus, the radar sensor perceives predictions that are not represented in the real world. The corresponding effect in this area is the multipath propagation. Furthermore, false negative detection occurs when the Signal-to-Noise Ratio (SNR) of the radar signal is too low and the radar sensor fails to detect the target. The true negative is the area range in which the radar sensor predicts correctly that there is not actual target present (Schlager et al., 2020).

Multipath propagation of a radar signal has been categorized into two types depending on the position of the resulting ghost target. Type 1 has referred to

propagation paths where the resulting ghost target appears on the same side as the radar and the actual target with respect to the reflecting surface. Additionally, type 2 has referred to propagation paths, where the ghost target appears on the other side of the reflective surface (Zhou et al., 2022). Multipath propagation can be described as follows, while waves operate in a particular spectrum, some surfaces can act like mirrors. Waves hitting such surfaces can be reflected at a certain angle in a different direction. This behavior causes the transmitted radar signals to take detours between the antenna and the target. This radar-specific property can therefore result in ghost targets in the measurement. Since these ghost targets have similar dynamics as the real targets, it is difficult to identify and eliminate them. In this paper, the multipath propagation effect for radar sensor in a specific SOTIF use case has been investigated.

3 CONCEPT AND METHODS

3.1 Sensor Activities

The procedure of SOTIF process are described in ISO 21448:2022 with eight key steps describe as, (i) functional and system specification, (ii) SOTIF related Hazard analysis and risk assessment (HARA), (iii) identification and evaluation of triggering events, (iv) functional modifications to reduce the SOTIF related risks, (v) defining of Verification and Validation (V&V), (vi) verification of the SOTIF known unsafe scenarios, (vii) verification of unknown unsafe scenarios and (viii) strategy for SOTIF related product release (ISO21448, 2022). For the evaluation of the radar sensor, identification and assessment of the triggering conditions is required. The functional modifications have been essential to reduce the SOTIF risks are considered with respect to a specific system specification. The radar sensors are often used for environment detection in HAD systems, such as Highway Chauffeur belongs to the SAE level 3 (Becker et al., 2020). The task of these sensors is, on the one hand, to detect objects at an early stage so that the system has enough time to react with a suitable maneuver. On the other hand, the sensors should detect objects with sufficient certainty so that the detected objects are not misinterpreted by the system.

As a first activity, radar sensor function has been defined as object detection in the highway while performing dynamic driving tasks. It is assumed that, the HAD system has the capability to activate and deactivate the sensor function as indented. Secondly, modeling scenarios based on the known system limitations

are investigated including the environmental conditions that may may exceed the system limitations and potentially could trigger hazardous situations. Lastly, functional modification to reduce the sensor related risks need to be identified based on the SOTIF related HARA such as, improvement of radar sensor's algorithms, modification of radar sensor location, implementation of detection by means of sensor disturbance and triggers warnings and uses of multiple sensors and/or sensor fusion.

3.2 Use Case

A use case has described a suite of related scenarios including additional information such as, functional range, desired behavior, system boundaries, environmental assumption and human operation. A scenario consists of several scenes and a sequence of scenes along with a specific situation, actions and events (ISO21448, 2022). ISO 21448 has detailed the definition of scene as, *a scene can include environmental elements (state, time, weather, lighting and other surrounding conditions), road infrastructure or internal elements (road or interior geometry, topology, quality, traffic signs, barriers, etc.) and objects/actors (static, dynamic, movable, interactions, manoeuvres if applicable)* (ISO21448, 2022). Moreover, according to ISO 21448 triggering condition is defined as, *a specific condition of a scenario that serves as an initiator for a subsequent system reaction contributing to either a hazardous behaviour or an inability to prevent or detect and mitigate a reasonably foreseeable indirect misuse* (ISO21448, 2022).

The HAD system is designed to be activated only on the highway as a chauffeur (Becker et al., 2020; IEC/TR63069, 2019). In addition, the highway must be divided by guardrails and have clear lane markings. However, there are some sections on the highways for which the system is not designed. For example, such sections can include construction sites, police checkpoints, toll booths and intersections. In this case, navigation at on-ramps and off-ramps is also not provided by the chauffeur system on the highway. Moreover, the system under consideration is not designed to operate in extreme weather conditions (e.g. heavy rain, fog) affects the system in such a way that it can no longer perform the driving task due to poor visibility.

A highway in Germany typically consists of two driving lanes and one shoulder lane. An essential component of highways is guardrails, that are used to enclose the road, to prevent vehicles to get off the road (FGSV, 2011). The desired behavior of the radar sensor is the detection of road users and determining the position, the velocity, and the angular posi-

tion relative to the ego-vehicle. A set of triggering conditions related to radar sensor has been described in (Becker et al., 2020). Among them is, *RS-4: the radar may not detect certain environmental feature with sufficient confidence, such as guardrails* (Becker et al., 2020). The RS-4 triggering condition has been examined in this paper using simulation-based testing to identify the sensor functional insufficiency and possible improvements.

The use case in this analysis has therefore been based on the likely use case of the chauffeur system for highways, where an ego-vehicle follows a lead vehicle on a highway. A radar sensor has been mounted on the ego-vehicle to perceive targets in the environment. Moreover, the effect of multipath propagation has been taken into account in the simulation to evaluate the radar sensor's ability to perceive the environment. The use case is depicted in the Figure 1 where, the radar has been mounted at the front the ego-vehicle (blue color) and the guardrail (bold black color) and the leading vehicle (orange color).

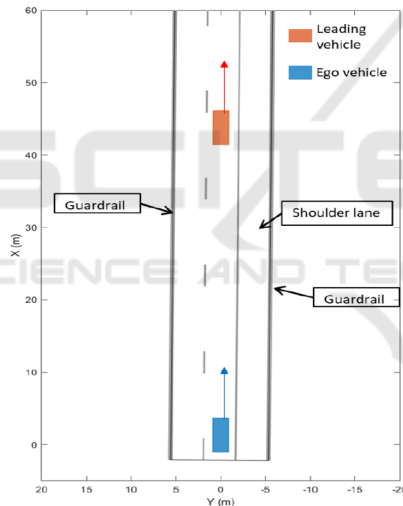


Figure 1: Use case concrete scenario modeling.

Table 1: Scenario modeling parameters.

Object	Measure	Value	Unit
Ego-vehicle	Velocity	27	m/s
Lead Vehicle	Velocity	27	m/s
Distance between vehicles	Distance	40	m
Simulation	Duration	4	s
Simulation	Sample time	0.1	s
Driving lane	Width	3.75	m
Shoulder lane	Width	3	m
Guardrail	Height	0.75	m

The relevant parameters of the scenario are shown in Table 1. The ego-vehicle equipped with a radar

sensor closely tracks the leading vehicle at the same speed in meter per second (m/s). The duration of the whole scenario is 4 seconds (s) and the sampling time is 0.1 s. The width of the lane and shoulder are chosen to represent a typical highway. The values used to set up the highway have been taken from road and transportation research association, Germany (FGSV, 2011).

3.3 Sensor Models

A statistical radar model and a physical radar model have been examined to evaluate sensor performance, and an use case scenario has been simulated. The radar effect (multipath propagation) has been evaluated with both sensor models to determine the potential functional insufficiency. As a by-product, potentially safety-critical triggering conditions have been achieved with respect to SOTIF and support FuSa as well for a HAD system.

The statistical radar sensor model provided by MATLAB corresponds to the medium-fidelity sensor models (Schlager et al., 2020). The statistical radar sensor model requires lower computational time than higher fidelity sensor models. The use of statistical radar sensor models make sense in the early beginning of the developing process, where first ideas and design trade-offs are being investigated. Due to the relatively low computational time, it is recommended to use this model also for longer simulations, but also test tracking and sensor fusion algorithms (Mathworks, 2022b). The sensor model does not consider signal processing and is only the fundamental for the principles of automotive radar expressed as (Mathworks, 2022f):

$$\text{Received power, } P_r = \frac{P_t * G_t * G_r * \lambda^2 * \sigma}{(4\pi)^3 * R^4 * L} \quad (1)$$

Where, G_t defines the gain of the transmitter. G_r indicates gain of the receiver. λ is the wavelength of the radar's operating frequency in meters (m). σ specify the radar cross section of the target in square meters (m^2) R display the range between radar sensor and target in meter (m). L shows the loss factor according to the transmitter and receiver and the propagation loss.

In radar range measurement, the maximum distance between the transceiver and the target depends on the received power P_r . Typically, the radar measurement contains noise, so the target can only be determined if the power at the receiver reaches a minimum power P_{rmin} . The minimum power P_{rmin} has to achieve a sufficient SNR to be distinguishable from the noise of the radar measurement. The resulting equation for the maximum range is as follows (Wolf, 2022):

$$\text{Maximum range, } R_{\max} = \sqrt[4]{\frac{P_s * G^2 * \lambda^2 * \sigma}{P_{r_{\min}} * (4\pi)^3 * L}} \quad (2)$$

Since the radar sensor uses electromagnetic waves that are traveling between the transceiver and the target, the time-of-flight (Δt) of the signal can be measured. Relating to the speed of light c and the mentioned Δt the distance R can be determined as follows (Herz, 2017):

$$\text{Distance, } R = \frac{\Delta t * c}{2} \quad (3)$$

The velocity on the other hand is determined by the Doppler effect as expressed in (Herz, 2017):

$$\text{Doppler frequency, } f_D = f_r - f_c = \frac{2 * f_t}{c} * v_r \quad (4)$$

The Doppler frequency F_D can be determined by the difference between the frequency of the transmitted signal f_t and the received signal f_r or with the corresponding radial velocity of the target v_r in m/s as unit. The I/Q stands for "In-phase" and "Quadrature". I/Q signals consist of two sinusoidal, which have identical frequencies but are 90° out of phase. I/Q signals are amplitude modulated and the amplitude of the resulting signal can be determined as follows (Podcast, 2022):

$$\text{Amplitude, } A = \sqrt{I^2 + Q^2} \quad (5)$$

Here, I and Q results regarding to the angular dependencies as $I = A * \cos\theta$ and $Q = A * \sin\theta$. The phase of the signal is (Podcast, 2022),

$$\text{Phase, } \theta = \tan^{-1} \frac{Q}{I} \quad (6)$$

The structure of the statistical sensor model based on the scheme of medium-fidelity has been presented in Figure 2.

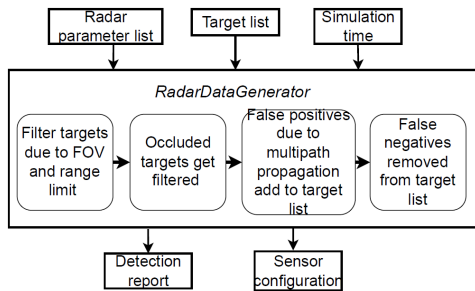


Figure 2: Block diagram of statistical radar model.

Figure 2 has the top three blocks showing the inputs required to create the radar sensor model. The middle block *RadarDataGenerator* containing four steps that the sensor model performs to process the input data. The bottom portion of Figure 2 represents the outputs provided by the radar sensor model.

The physics-based radar sensor model has also been observed to correspond to medium accuracy sensor models, such as the radar sensor model presented for statistical radar model. The difference between the statistical radar sensor model and the physics-based radar model is that the latter generates sampled I/Q signals. These I/Q signals are converted into target detection. In a addition, the physics-based model also takes into account the transmitted waveform, the propagation of the signal in the simulated environment, reflections from the targets, and signals received at the receiving facility.

The waveform of the modeled radar transceiver is a pulse Doppler radar waveform. To set the waveform, the Pulse Repetition Frequency (PRF), which is calculated from the Doppler resolution Δf in this sensor model, and the number of pulses (N) has to be determined as follows (Gamba, 2020; Mathworks, 2022i):

$$\text{Pulserepetitionfrequency, PRF} = \Delta f * N_p \quad (7)$$

$$\text{Magnitude, } N_p = \frac{1}{\Delta f * T_p} \quad (8)$$

The magnitude N_p , represents the number of pulses, which are sent out per one measurement and is calculated as follows, where Δf is Doppler resolution and T_p the pulse width.

Figure 3 depicts the structure of the physics-based radar model.

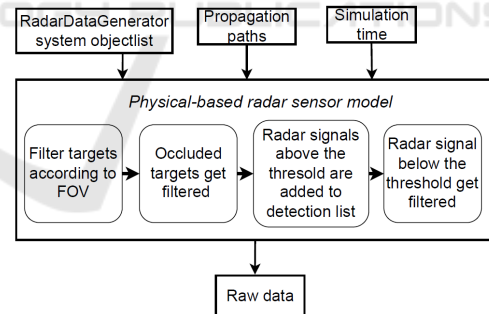


Figure 3: Block diagram of physical-based radar model.

The physics-based radar sensor model uses MATLAB's system object *radarTransceiver* to generate I/Q signals in the time domain (Mathworks, 2022i). This virtual radar transceiver can be generated by the equivalent *radarDataGenerator*, that is also needed to create the statistical radar sensor model. Consequently, it is a part of the input for the physically based radar sensor model. The propagation paths have been computed in an auxiliary function provided by MATLAB. The output of this function provides information in a detailed structure of every propagation path. The path of the signal is measured starting at the

transmitter and ending at the receiver. The path loss L in decibel of the waveform λ which propagates over the distance R in meters (m) (Mathworks, 2022c)

$$Pathloss, L = 20 \log_{10} \left(\frac{4\pi R}{\lambda} \right) \quad (9)$$

The reflection coefficient describes a specific magnitude of the propagation path depending on how many times the signal bounces off a reflective surface. RCS defines the reflection coefficient surface. If the signal bounces off a surface once or twice, the reflection coefficient becomes smaller. It is calculated as follows, with the corresponding radar cross section of the target and the wavelength (Mathworks, 2022a).

$$Reflectioncoefficient, Ref_{coeff} = \frac{4\pi}{\lambda^2} * RCS \quad (10)$$

Finally, the last field of the structure contains the Doppler shift of the received signal, which is calculated by the radial velocity (v_r) of the target, given in meters per second and the wavelength λ . The resulting Doppler frequency Δf is given in hertz (Mathworks, 2022h).

$$Dopplerfrequency, \Delta f = \frac{v_r}{\lambda} \quad (11)$$

The physics-based radar sensor model has used all propagation paths as shown in Figure 4, as input for the *radarTransceiver* system object. The resulting output consists of the corresponding sampled I/Q signals based on the related signal processing settings and calculations.

Figure 5 has represented a two-dimensional data set with local and global maxima and local and global minima from three-dimensional surface plot (x-y plane is defined by X and Y and Z as surface height) (Liske, 2022). For example, the local maxima has indicated by the values at the highest point of a curve within a certain range. The highest and lowest values of the entire data set has been manifested by the global maximum and global minimum.

The resulting local maxima inclusively the global maximum represents the SNR of the potential targets. With the location of each local maxima in the data set, the relative position of the target can be determined. This has been accomplished with the resulting location of the SNR in the corresponding fast-time domain. Since the fast-time samples represents the range bins, the determined location of the local maxima in the fast-time domain is used to identify the range. The determination of local maxima is also used for identifying the azimuth angle of the targets. Due to the phase shift beam-forming, each scanning angle can be considered. Therefore, the position of the local maxima in the second dimension of the radar data

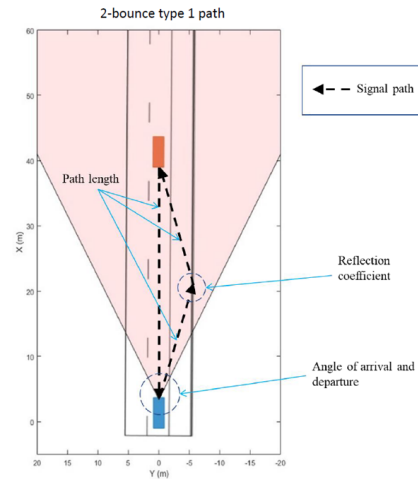


Figure 4: Propagation path of 2-bounce type 1 properties.

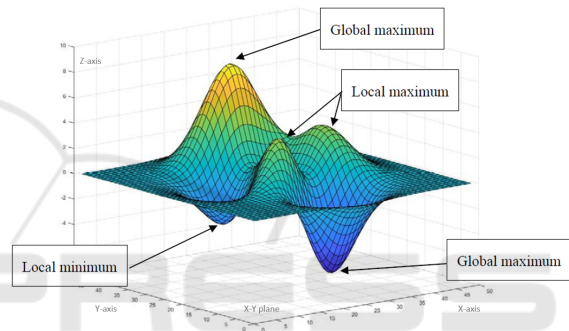


Figure 5: Representation of global and local maxima/minima in a 2D data set (Liske, 2022).

cube indicates the corresponding angle where the target is located (Mathworks, 2022e). The local maxima has been presented in both sensor models as simulation outcomes.

4 SIMULATION-BASED TESTING IMPLEMENTATION

4.1 Implementation

The radar-related visualization in this study consists of the Field Of View (FOV) and radar detection represented as colored dots. Black colored dots are true positive detection, meaning they represent detection that have the associated signal transmitted directly between the radar and the target. The orange and red dots indicate which propagation path the detection is based on, as displayed in Figure 6.

The structure of the implementation process for the statistical radar sensor model in MATLAB is demonstrated in Figure 6. MATLAB provides an

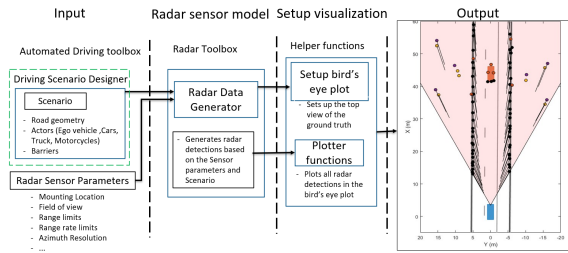


Figure 6: Implementation of statistical radar sensor model.

application, which is called “Driving Scenario Designer” (Mathworks, 2022g; Mathworks, 2022d). This application has been included from the automated driving toolbox and provides a graphical interface to build a scenario. The modeled scenario has been exported as a MATLAB function and implemented in the radar sensor model with the help of Equations (1)-(6). The Radar data generator, a system object provided by the radar toolbox generates the detection. These detection are based on the defined radar sensor parameters and the scenario parameters. The output of the Radar data generator is used by so-called “helper functions” to output the visualization of the scenario with the corresponding radar detection (Mathworks, 2022g).

The physics-based radar sensor model can be seen as the extension of the statistical radar sensor model. A radar transceiver is modeled to generate I/Q signals in the time domain that are represented the returning signals. These returning signals are generated based on the possible propagation paths which results between the environment and the radar.

In Figure 7 the *radartransceiver* system object is included in the MATLAB’s radar toolbox (Mathworks, 2022b). To process the resulting radar data cube, which contains the sampled I/Q signals, the MATLAB’s phased array system toolbox is considered. This toolbox includes *radarDopplerResponse* system object and the *phaseShiftBeamformer* system object. The former one is used to process the range by Equation (2) and Doppler information by Equation (11), that is included in the radar data cube and the latter one is used to vary the scanning angle to extract the angle information out of the data cube (Mathworks, 2022e).

Further, the resulting raw data can be used to visualize the distribution of the SNR in the measurement in an appropriate range-angle map, which is also represented in Figure 7.

4.2 Radar Sensor Setup and Simulation

The ego-vehicle in the use case scenario has been equipped with a forward-facing mono-static radar.

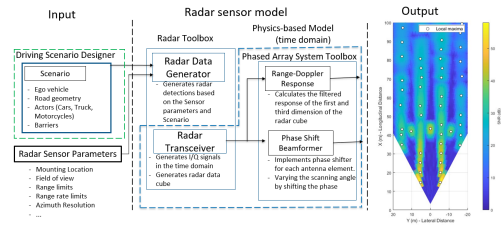


Figure 7: Implementation of physical-based radar sensor model.

The sensor’s transmitter and receiver are therefore located in one place. Currently, the radar sensors used to implement advanced driver assistance systems and automated driving functions operate at a frequency of 76 GHz to 77 GHz (Mathworks, 2022f). The radar sensor is located 0.2 m above the ground in the center of the front bumper of the ego-vehicle. According to (Ziegler et al., 2014), the FOV of the radar and the maximum detection range are based on the setup for the long-range radar used for the Bertha Benz test vehicle. The azimuth angle resolution for conventional radar sensors is given between 1.5° and 4° according to (Yu et al., 2022). In the radar sensor setup presented in this paper, the azimuth angle is set to 2° to achieve a higher resolution in the angle measurement. The range resolution is set to 2.5 m and thus to a smaller size corresponding to the length of a vehicle. Finally, the limits of the range rate are set to the range corresponding to the maximum allowable operating speed of the driving function of 100 m/s. The radar sensor has the ability to detect the varying speeds of the targets in steps of 0.5 m/s within the distance limits as listed in Table 2.

Table 2: Radar model parameters.

Object	Measure	Value	Unit
Center frequency	Frequency	77	GHz
Sensor Mounting	Height	0.2	m
FOV	Azimuth/ Elevation	56/9	deg
Maximal Range	Distance	60	m
Range rate limits	Velocity Elevation	-100... 100	m/s
Angle resolution	Azimuth angle	2	deg
Range resolution	Distance	2.5	m
Range rate resolution	Velocity	0.5	m

The statistical radar sensor model has been applied to simulate the scenario described in section 3. A snapshot of a scene from the scenario is viewed in Figure 8. This snapshot shows the overhead view of the scene, also referred to as a bird’s eye view. Fig-

Figure 8 has primarily shown the ground truth data of the environment, which includes the road, guardrails, and the two vehicles (ego-vehicle: blue and leading vehicle: orange). The radar sensor's coverage area, which is the area defined by the specific FOV, and the maximum coverage area are also illustrated in Figure 8.

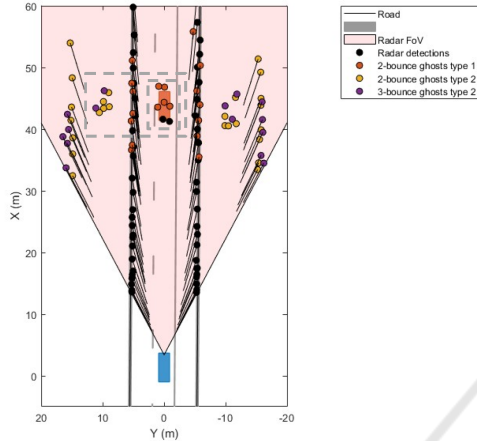


Figure 8: Top view of the scene (statistical radar sensor model).

The statistical radar sensor model generates a report that contains information about the relative position of each detection. Depending on the position, the detection points are plotted as dots in the bird's eye view, as shown in Figure 8. Within the radar sensor's detection area, the radar detection points are shown as black and colored dots as visible in Figure 8.

The physics-based sensor model includes the radar-specific waveforms in the time domain and the corresponding signal processing part. Since the resulting output of this type of sensor model consists of raw data, the information has to be interpreted differently than for example the statistical radar sensor model. This radar-specific raw data has included range, angle, and Doppler information. To represent the position of targets in a bird's eye view, the processed range and angle information has been used to create the visualization. The architecture of the physics-based sensor model was described in the previous section 3.

The Figure 9 provides a bird's eye view of the distribution of the SNR with the support of radar received power that has been calculated with the support of Equations (1), (9) and (10), together with the corresponding local maxima. Thus, the targets based on the generated I/Q signals and the corresponding signal processing can be performed. The ground truth data has been presented by Figure 9 for a specific use case scenario.

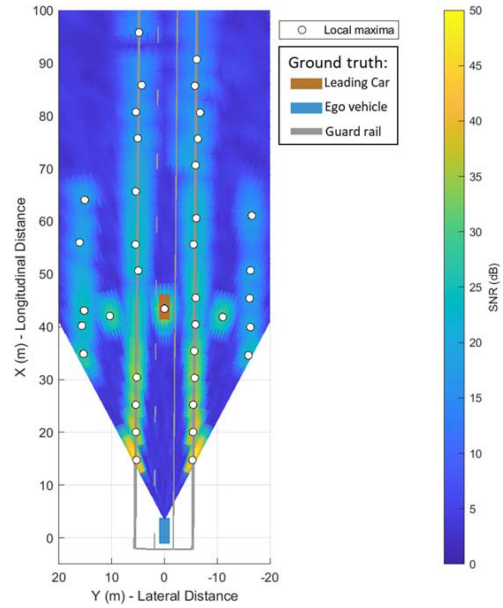


Figure 9: Top view of the scene (physical-based radar sensor model).

4.3 Results and Discussions

Since the statistical radar sensor model and the physics-based radar sensor model are subject to different architectures, the output measurement varies in some respects as marked in Figure 10. Both sides of the Figure 10 reveal a snapshot of the scenario at time 0.2 s.

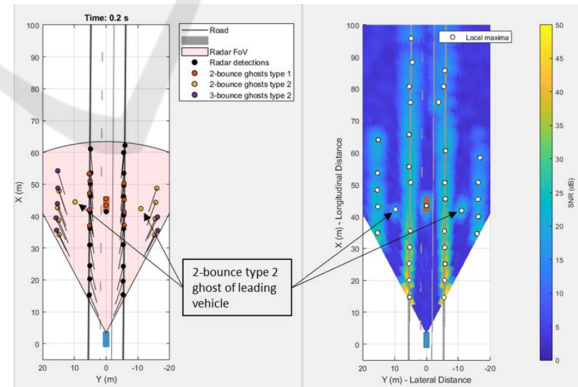


Figure 10: Snapshot of both radar sensor models.

The maximum unique detection range has been observed in Figure 10 for both sensor models. In one hand, the statistical radar sensor model sets its detection range only to the maximum range value as defined in Table 2. On the other hand, physics-based radar sensor model has wide range. The maximum range is determined by the *PRF*. The *PRF* is calculated through Equation (7) and Equation (8). The *PRF*

depends on the number of pulses that are sent out per measurement and the range rate resolution, which is also defined in Table 2.

Table 3: Relative position and SNR for statistical radar model.

Properties	Δx	Δy	SNR
Ground truth	42.41 m	-0.05 m	-
Desired detection	41.38 m	-0.03 m	20.67 dB
2-bounce type 1 ghost	45.42 m	0.07 m	17.35 dB
2-bounce type 2 ghost left	44.45 m	9.76 m	19 dB
2-bounce type 2 ghost right	42.34 m	-10.92 m	18.81 dB

Table 3 illustrates the measurement data of desired detection, ghost detection due to multipath propagation, and ground truth data of the leading vehicle. The ground truth is presented as the actual relative position (Δx , Δy) and SNR by the measurement data provided by the simulation as recorded in Table 3. For example, The SNR rate of the desired detection has been achieved by statistic radar model is ≈ 20 dB. The values of the measurement according to the desired detection almost correspond to the ground truth data. This is an evidence that the black dots represent adequate detection of the target by the radar. The red dots are 2-bounce type 1 ghost images, meaning that the radar signal bounces off a reflective surface on its way to the target. Reflection off a surface results in a longer time of flight for the radar signal and thus a greater relative distance.

An illustration of a pie chart in Figure 11 contains all the dynamic detection within the simulation time of 4 s. Since the sample time of the simulation is 0.1 s, the resulting simulation steps equal to 40. Therefore, in every simulation step, the distribution of desired detection and ghost detection is evaluated and added up.

The pie chart in Figure 11 sketches the percentage distribution of ghost detection. The greatest proportion has been covered by the 2-bounce path type 2 ghosts with $\approx 36\%$. The 3-bounce path type 2 ghost has the lowest proportion with about half of the 2-bounce ghosts with $\approx 18\%$. The area has been covered by 2-bounce type 1 ghosts and desired detection is $\approx 21\%$ and $\approx 22\%$, respectively. According to this analysis, the amount of ghost/false detection is relatively high.

The simulation results based on the physical-based radar has been presented in Table 4 with respect to the outcomes as relative position (Δx , Δy) and SNR.

Average clutter distribution of true and ghost detections within 4 sec. simulation time

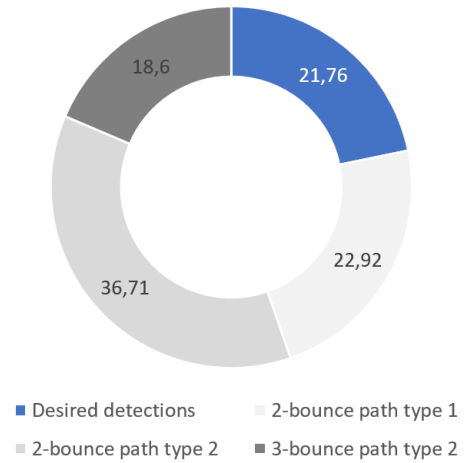


Figure 11: Percentage distribution of detection for statistical radar sensor model.

The desired detection rate has SNR value of ≈ 25 dB for physical-based radar model. Table 3 and Table 4 have represented the relative position and the SNR of the desired detection and the ghost detection of the leading vehicle considering the outcomes of statistical radar model and physical-based radar model accordingly.

Table 4: Relative position and SNR for physical-based radar model.

Properties	Δx	Δy	SNR
Ground truth	42.41 m	-0.05 m	-
Desired detection	41.40 m	0 m	25.02 dB
2-bounce type 1 ghost	-	-	-
2-bounce type 2 ghost left	42.21 m	9.68 m	17.66 dB
2-bounce type 2 ghost right	41.85 m	-10.02 m	24.01 dB

In this simulation the position of the radar detections is compared with the ground truth. Additionally, If a local maxima does not cover an object's ground truth, it will be considered as ghost target. According to the simulation results from physical-based radar sensor model, true detection is performed $\approx 49\%$ and able to detect the leading vehicle approximately $\approx 94\%$ as exhibited in Figure 12.

The results have been represented on the basis of a "true" or "false" detection. This is done by checking whether a local maximum covers an object of ground truth. If this is the case, it can be assumed that the radar is detecting the object correctly, and the detec-

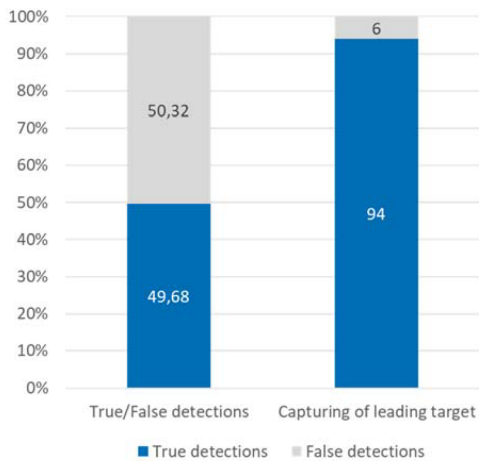


Figure 12: Detection of leading vehicle by physical-based radar sensor model.

tion in this case is called a "correct detection". All other detections that do not cover a ground truth object are referred to as "false detection".

Furthermore, the simulation results validate the detection of the leading vehicle by the radar sensor throughout the simulation. Since the methods described in the previous subsection consider the ground truth object covered by a local maximum, it is possible to check whether the radar sensor detects the leading vehicle during the entire simulation.

4.4 Sensor Performance Improvement

From the simulation results of the statistical radar sensor model, the highest proportion of ghost targets are the 2-bounce type 2 ghosts. The analysis of the SNR of the physics-based radar sensor model has shown that such ghost detection can have characteristics like real detection. Moreover, the physics-based radar sensor model has yielded as a result that the leading vehicle is captured most of the simulation time. According to these results, a filter development has great emphasis that can identify 2-bounce and 3-bounce type 2 ghosts. Hence, a filter has been modeled and tested for the use case.

The developed filter has focused only on detection after moving objects. Since the radar sensor in the physics-based model almost always detects the leading vehicle, the 2-bounce type 1 ghosts are disregarded in this case. For Type 2 ghost have been located outside the road. Because the angle of the returning signal results from the signal bouncing off the guardrail as it returns to the sensor after reflecting off the vehicle ahead, these type 2 ghost images are projected onto the other side of the guardrail. The concept flow diagram of the developed filter has been

laid-out in Figure 13. The following flow diagram in Figure 13 has conveyed the rough structure of the algorithm.

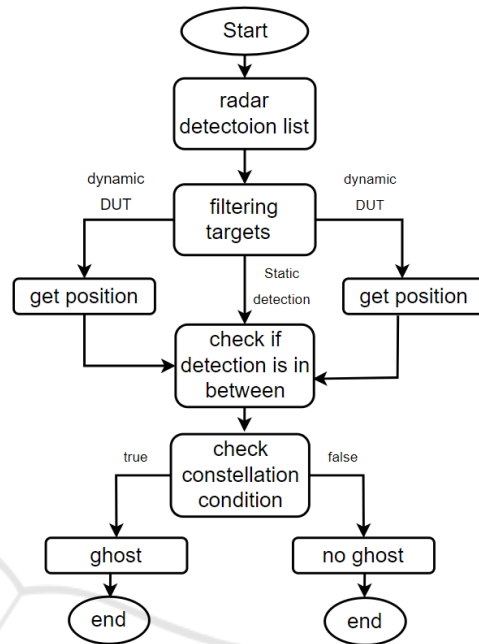


Figure 13: Flow diagram of the filter algorithm.

A reduced amount of type 2 ghosts points has been the after-effect of the developed filter for statistic radar model and appeared in the Figure 14. The left and right sides of Figure 14 have detection points with type 2 ghost points and the corresponding filtered type 2 ghost points.

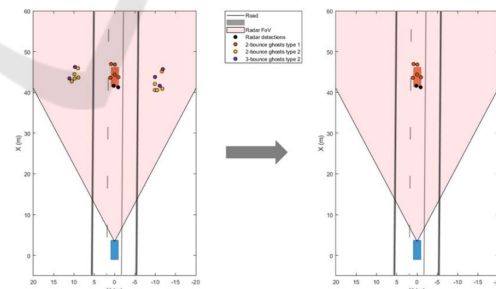


Figure 14: Radar detection without filter (left). Radar detection with filter (right).

Due to the fact that the detection list of the statistical radar sensor model contains detailed data about each detection, only the specific raw data such as relative velocity and relative position have been used to implement the filter. Thus, it will be possible to apply this filter to the physics-based radar sensor model as well. The first step, as shown in Figure 13, is to filter the static objects in the radar detection list. The

next step is to select a dynamic detection, called a Detection Under Test (DUT). This DUT has been tested next to determine if it is a type 2 ghost. Another dynamic detection has to be selected from the detection list, which can also be referred to as Detection Under Comparison (DUC). Next, a check has been made to verify whether there is a static detection between the DUT and the DUC. If this is the case, it has been indicated that there is a guard rail between the two detections, indicating that the DUT under consideration is a Type 2 ghost.

5 CONCLUSION

In this paper, a comprehensive methodology for simulation-based testing of an automotive radar for a specific SOTIF use case scenario has been presented in a systematic manner. This study has provided a simulation-based test concept to identify the performance insufficiency of radar models with respect to a use case applicable in HAD systems like highway chauffeur. For simulating the defined use case scenario two kinds of radar models are applied.

Moreover, multipath propagation effect for a radar sensor has been evaluated by examining both statistical and physical-based radar models. Therefore, possible triggering conditions has been realized to support the SOTIF of HAD systems. The statistical radar model has been used to analyse the occurrence of ghost targets due to the multipath propagation effect which leads to an inaccurate perception of the radar sensor. The simulation results of the statistical radar sensor model have illustrate that over 75% of the detection representing the leading vehicle are ghost detection and thus false positives. The majority of ghosts are 2-bounce type 2 ghosts. Additionally, physics-based radar sensor model has generated time-domain I/Q signals with signal processing like range Doppler processing and phase shift beamforming. Therefore, physics-based radar sensor model has more detailed representation of radar sensors and has been used to validate the simulation outcomes of the statistical radar sensor model.

Furthermore, a filter has been developed to reduce the type 2 ghost detection as a remedy of functional insufficiency of a radar model in the focus of the reflection on guardrails. The improved detection of the radar with the filer has been presented as an upshots of this study.

The focus of future work can be to implement the physics-based radar sensor model in a more complex environment where more environmental influences and reflective surfaces are present. In addi-

tion, the presented simulation-based testing approach can be used to investigate more use cases considering multipath propagation to support the verification and validation of a radar sensor.

REFERENCES

- Becker, C. J., Brewer, J. C., and Yount, L. J. (2020). Safety of the intended functionality of lane-centering and lane-changing maneuvers of a generic level 3 highway chauffeur system.
- Berk, M. and Schubert, O., Kroll, H.-M., Buschardt, B., and Straub, D. (2020). Assessing the safety of environment perception in automated driving vehicles. 8 (1):49–74.
- FGSV (2011). Guidelines for the design of motorways (raa). https://www.fgsv-verlag.de/pub/media/pdf/202_E_PDF.v.pdf.
- Gamba, J. (2020). *Radar Signal Processing for Autonomous Driving*. Springer Singapore, Singapore, 1st edition.
- Herz, G. (2017). Development of a radar sensor behavior model for validation of advanced driver assistance systems.
- Herz, G., Schick, B., Hettel, R., and Meinel, H. (2019). Sophisticated sensor model framework providing realistic radar sensor behavior in virtual environments.
- IEC/TR63069 (2019). Industrial-process measurement, control, and automation - framework for functional safety and security. <https://webstore.iec.ch/publication/31421>.
- ISO21448 (2022). Road vehicles — safety of the intended functionality. <https://www.iso.org/standard/77490.html>.
- ISO26262 (2018). Road vehicle — functional safety, part 1 to part 13. <https://www.iso.org/standard/43464.html>.
- Khatun, M., Caldeira, G., Jung, R., and Glaß, M. (2021a). An optimization and validation method to detect the collision scenarios and identifying the safety specification of highly automated driving vehicle. In *21st International Conference on Control, Automation and Systems (ICCAS)*, pages 1570–1575.
- Khatun, M., Caldeira, G., Jung, R., and Glaß, M. (2021b). A systematic approach of reduced scenario-based safety analysis for highly automated driving function. In *7th International Conference on Vehicle Technology and Intelligent Transport Systems*. Scitepress.
- Khatun, M., Glaß, M., and Jung, R. (2020). Scenario-based extended hara incorporating functional safety and sotif for autonomous driving. *30th European Safety and Reliability Conference*.
- Leither, A., Watzenig, D., and Ibanez, J. (2020). *Validation and Verification of Automated Systems*. Springer Nature Switzerland AG., European Union, 1st edition.
- Liske, M. (2022). Master thesis: Simulation-based testing to improve the sensor limitations for a sotif use case scenario. In *Masther Thesis*. Institute for Advanced Driver Assistance Systems and Connected Mobility-Kempten University of Applied Sciences.

- Martin, H., Winkler, B., Grubmüller, S., and Watzenig, D. (2019). Identification of performance limitations of sensing technologies for automated driving. In *2019 IEEE International Conference on Connected Vehicles and Expo (ICCVE)*, pages 1–6.
- Mathworks (2022a). aperture2gain: Convert effective aperture to gain. <https://de.mathworks.com/help/phased/ref/aperture2gain.html?searchHighlight=%20ap>.
- Mathworks (2022b). Create physics-based radar model from statistical model. <https://de.mathworks.com/help/radar/ug/radar-model-abstract-level.html>.
- Mathworks (2022c). fspl: Free space path loss. [https://de.mathworks.com/help/phased/ref/fspl.html#:~:text=Description,-example&text=L%20%3D%20fspl\(%20R%20%2C%20lambda%20\)%20returns%20th](https://de.mathworks.com/help/phased/ref/fspl.html#:~:text=Description,-example&text=L%20%3D%20fspl(%20R%20%2C%20lambda%20)%20returns%20th).
- Mathworks (2022d). Introduction to statistical radar models for object tracking. <https://www.mathworks.com/help/fusion/ug/introduction-to-radar-for-object-tracking.html>.
- Mathworks (2022e). Radar data cube concept. https://de.mathworks.com/help/phased/gs/radar-data-cube.html?searchHighlight=RADAR%20data%20cube&s_tid=srchtitle_RADAR%252.
- Mathworks (2022f). Radar equation: Radar equation theory. <https://de.mathworks.com/help/radar/ug/radar-equation.html>.
- Mathworks (2022g). radardatagenerator: Generate radar detections and tracks. <https://de.mathworks.com/help/radar/ref/radardatagenerator-system-object.html>.
- Mathworks (2022h). speed2dop: Convert speed to doppler shift. <https://de.mathworks.com/help/phased/ref/speed2dop.html?searchHighlight=speed2do>.
- Mathworks (2022i). time2range: Convert propagation time to propagation distance. <https://de.mathworks.com/help/phased/ref/time2range.html?searchHighlight=time%25>.
- Mazzega, J. (2019). Pegasus method: An overview. *PEGASUS Symphony*.
- Parker, M. (2017). Chapter 20-automotive radar with contributions by ben esposito. In Parker, M., editor, *Digital Signal Processing 101 (Second Edition)*, pages 253–276. Newnes, 2nd edition.
- Podcast (2022). Understanding i/q signals and quadrature modulation: Chapter 5 - radio frequency demodulation. <https://www.allaboutcircuits.com/textbook/radio-frequency-analysis-design/radio-frequency-demodulation/understanding-i-q-signals-and-quadrature-modulation/>.
- SAEJ3016 (2021). Taxonomy and definitions for terms related to driving automation systems for on-road motor vehicles. https://www.sae.org/standards/content/j3016_202104/.
- Schlager, B., Muckenhuber, S., Schmidt, S. and Holzer, H., Rott, R. and Maier, F. M., Saad, K., Kirchengast, M., Stettinger, G., Watzenig, D., and Ruebsam, J. (2020). State-of-the-art sensor models for virtual testing of advanced driver assistance systems / autonomous driving functions. *SAE International Journal of Connected and Automated Vehicles*, 3(3):233–261.
- UL4600 (2022). Standard for evaluation of autonomous products. <https://ul.org/UL4600>.
- Valdez Banda, O. A. and Goerlandt, F. (2018). A stamp-based approach for designing maritime safety management systems. *Safety Science*, 109:109–129.
- Winner, H., Hakuli, S., Lotz, F., and Singer, C. (2015). *Handbuch Fahrerassistenzsysteme: Grundlagen, Komponenten und Systeme für aktive Sicherheit und Komfort*. Springer Vieweg Wiesbaden, Wiesbaden, 3rd edition.
- Wolf, C. (2022). The radar range equation, argumentation/derivation. <https://www.radartutorial.eu/01.basics/The%20Radar%20Rang%20Equation.en.html>.
- Yu, W., Li, J., Peng, L.-M. and Xiong, X., Yang, K., and Wang, H. (2022). Sotif risk mitigation based on unified odd monitoring for autonomous vehicles. *Journal of Intelligent and Connected Vehicles*.
- Zhou, Y., Liu, L., Zhao, H., López-Benítez, M., Yu, L., and Yue, Y. (2022). Towards deep radar perception for autonomous driving: Datasets, methods, and challenges. *Sensors*, 22(11).
- Ziegler, J., Bender, P., Schreiber, M., Lategahn, H., Strauss, T., Stiller, C., Dang, T., Franke, U., Appenrodt, N., Keller, C. G., Kaus, E., Herrtwich, R. G., Rabe, C., Pfeiffer, D., Lindner, F., Stein, F., Erbs, F., Enzweiler, M., Knöppel, C., Hipp, J., Haueis, M., Trepte, M., Brenk, C., Tamke, A., Ghanaat, M., Braun, M., Joos, A., Fritz, H., Mock, H., Hein, M., and Zeeb, E. (2014). Making bertha drive—an autonomous journey on a historic route. *IEEE Intelligent Transportation Systems Magazine*, 6(2):8–20.